

Slow Motions in Nondeuterated Proteins: Concerted Chemical Shift Modulations of Backbone Nuclei

J. Wist¹, C. Perazzolo¹, and G. Bodenhausen²

¹Institut des Sciences et Ingénierie Chimiques, Ecole Polytechnique Fédérale de Lausanne, Lausanne, Switzerland

²Département de Chimie, Associé au CNRS, Ecole Normale Supérieure, Paris, France

Received October 5, 2004

Abstract. A simple method designed to measure autorelaxation rates of double- and zero-quantum coherences $DQC/ZQC\{C'N\}$ involving a carbonyl C' and the neighboring amide N nucleus in protein backbones provides valuable insight into slow motions in spite of interference both from the attached amide proton H^N and from remote protons such as H^α in nondeuterated proteins. The method has been applied to human ubiquitin.

1 Introduction

It is well known that fluctuations of isotropic chemical shifts caused by slow exchange between energetically accessible conformations contribute to the transverse relaxation of nuclei like nitrogen-15 [1, 2] and carbon-13 [3].

Slow correlated fluctuations of isotropic chemical shifts of a selected pair of nuclei can provide detailed evidence for slow motions in proteins and other biomolecules. Along with effects of chemical shift anisotropy (CSA), these fluctuations contribute to differential line broadening between zero- and double-quantum coherences (ZQC and DQC) involving the selected pair of nuclei. So far, four complementary methods have been developed in our laboratory. Two of them enable the measurement of CS–CS cross-correlated rates, i.e., the sum of isotropic chemical shift modulations (CSM/CSM) and anisotropic (CSA/CSA) contributions. In nucleic acids, one can monitor the auto- and cross-correlated relaxation of double- or triple-quantum coherences $DQC\{N^D N^A\}$ or $TQC\{N^{DH_{imino}} N^A\}$ involving the Watson–Crick donor and acceptor nitrogens N^D and N^A , as well as the hydrogen-bonding imino protons [4, 5]. For proteins, it is instructive to measure the relaxation properties of zero- and double-quantum coherences $DQC/ZQC\{C^\alpha C^\beta\}$ involving two neighboring carbon-13 nuclei belonging to the side-chains of amino acids [6, 7]. In some residues, the measured cross-correlated

CS–CS relaxation rates were significantly larger than expected, suggesting the presence of CSM/CSM contributions. More refined information can be obtained by multiple refocusing (CPMG) [8, 9] of ZQC and DQC, since only the CSM/CSM contribution will be attenuated with increasing pulse repetition rates. Thus, measurements of CS–CS rates as a function of pulse repetition rates enable the separation of CSM/CSM (rank 0 interactions) from CSA/CSA (rank 2 interactions). A TQC/SQC{C'NH^N} method involving a carbonyl C' nucleus, the neighboring amide N nucleus, and the attached amide proton H^N, can provide evidence of slow backbone motions [10]. More recently, a DQC/ZQC{NH^N} experiment involving only an amide N nucleus and its attached proton H^N has been shown to provide useful information [11]. Unfortunately, all aforementioned methods are best applied to deuterated proteins, because remote protons such as H^α, different from amide protons H^N, interfere partly through homonuclear scalar couplings such as $J(H^N H^\alpha)$ and partly through contributions to the relaxation of multiple-quantum coherences. Unfortunately, deuteration implies severe restrictions on the choice of samples.

In this paper, we show that DQC/ZQC experiments involving only C' and N nuclei (instead of the TQC/SQC experiments described previously [10]) can be used for the identification of residues experiencing conformational exchange, in spite of interferences both from the attached H^N proton and from remote protons such as H^α, provided that these dipolar contributions do not vary significantly from one residue to another.

2 Theory

The earlier TQC/SQC{C'NH^N} method [10] was designed to measure the difference $\Delta R(\text{TQC/SQC})$ in autorelaxation rates of TQC(C'₊N₊H_x^N) and three-spin SQC(C'₊N₋H_x^N). In this paper, we shall report measurements of rates $\Delta R(\text{DQC/ZQC})$ which are obtained from the autorelaxation rates of DQC(C'₊N₊) and ZQC(C'₊N₋). Both rates $\Delta R(\text{TQC/SQC})$ and $\Delta R(\text{DQC/ZQC})$ can be predicted from a common set of equations, although the magnitudes of the dipolar contributions differ:

$$\Delta R = 2(R^{\text{CS-CS}} + R^{\text{DD/DD}}),$$

where

$$R^{\text{CS-CS}} = R^{\text{CSA/CSA}}(C'_{i-1}N_i) + R^{\text{CSM/CSM}}(C'_{i-1}N_i)$$

and

$$R^{\text{DD/DD}} = R^{\text{DD/DD}}(C'_{i-1}H_i^N / N_i H_i^N) + \sum_k R_k^{\text{DD/DD}}(C'_{i-1}H_k^{\text{ali}} / N_i H_k^{\text{ali}}). \quad (1)$$

The cross-correlation rate $R^{\text{CSA/CSA}}(C'_{i-1}N_i)$ is due to the concerted modulations of the anisotropic chemical shifts induced by molecular tumbling, while the cross-

correlation rate $R^{\text{CSM/CSM}}(C'_{i-1}N_i)$ is due to concerted modulations of the isotropic chemical shifts caused by internal motions. The CSA/CSA rate cannot be affected by external manipulations without affecting at the same time the CSM/CSM rate, whilst the latter contribution can be quenched by spin-locking or by multiple-refocusing sequences with high repetition rates if the internal motions are not too fast.

In deuterated proteins the second term of Eq. (1) becomes negligible due to the substitution of aliphatic protons by deuterons. For TQC/SQC{C'NH^N} rates, the first term can also be neglected in slowly tumbling macromolecules, since the $J(0)$ contribution of $R^{\text{DD/DD}}(C'_{i-1}H_i^N/N_iH_i^N)$ vanishes if the amide proton is included in the coherence. Thus only the CSA/CSA and the CSM/CSM interactions contribute significantly to the differential line-broadening between TQC and SQC in deuterated proteins:

$$\Delta R(\text{TQC/SQC}) = R(C'_+N_+H_x) - R(C'_+N_-H_x).$$

In nondeuterated proteins, on the other hand, if the amide proton is included in the coherence, this introduces perturbations resulting from homonuclear scalar couplings with neighboring H^α protons. Measurements of DQC and ZQC decays (instead of TQC and SQC decays) are therefore preferable since they do not suffer from homonuclear couplings.

In nondeuterated samples, dipolar interference effects due to H^α protons contribute to the differential line-broadening, so that the rates

$$\Delta R(\text{DQC/ZQC}) = R(C'_+N_+) - R(C'_+N_-)$$

contain contributions from both dipolar terms of Eq. (1).

3 Materials and Methods

Uniformly ¹³C/¹⁵N/²D-enriched ubiquitin and uniformly ¹³C/¹⁵N-enriched ubiquitin were obtained commercially (VLI). Each protein was dissolved in 10% D₂O–90% H₂O with phosphate buffer at pH 6.7 to a concentration of 1.5 mM. The pulse sequence for measuring $\Delta R(\text{DQC/ZQC})$ (Fig. 1) is closely related to the experiments of Zuiderweg and co-workers [12], and to the sequence used for measuring $\Delta R(\text{TQC/SQC})$ [10]. The data were acquired at 300 K on a Bruker DRX-600 spectrometer equipped with a triple resonance TBI probe with triple axes gradients. The experimental time for each 2-D experiment was 2 h. Each matrix consisted of 128 and 1024 points in the t_1 and t_2 dimensions. The data were processed by the GNU Package NmrPipe/NmrDraw/NlinLS [13]. Each dimension was apodized by a 90° phase-shifted squared sine-bell window function and zero-filled once. Decay curves were sampled at 5 to 6 values of τ_m (Fig. 2) Duplicates were recorded for the first and third point of each decay. Errors of the apparent decay rates were estimated by Monte Carlo analysis [14]. Errors in ΔR were obtained by error propagation.

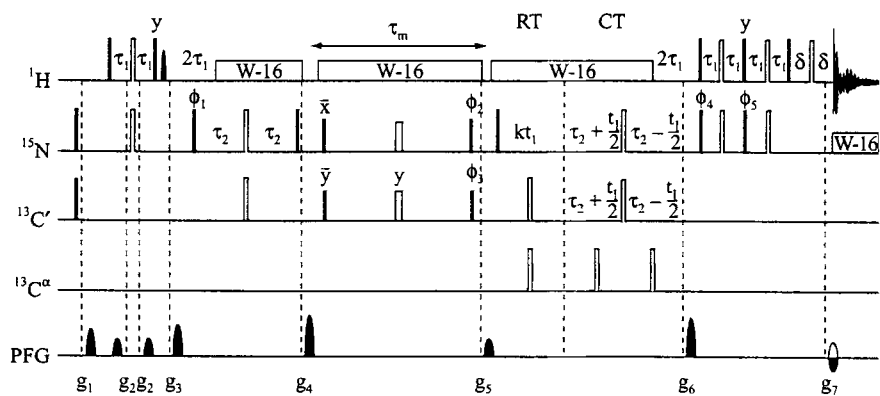


Fig. 1. Pulse sequence designed to measure the autorelaxation rates of DQC(C'_+N_+) and ZQC(C'_+N_-). Black and white rectangles represent $\pi/2$ and π pulses. All pulses are applied along the x -axes, unless specified otherwise. The ^1H , ^{15}N , ^{13}C carriers are centered at 4.7, 118 and 175 ppm, respectively. 90° and 180° pulses are applied to ^{13}C with field strengths of $\Delta/\sqrt{15}$ and $\Delta/\sqrt{3}$, Δ being defined as the difference in hertz between the centers of the C' and C^α regions ($\Delta = 17.6$ kHz at 600 MHz). Pulses applied to C^α are phase modulated. During the mixing time τ_m , the evolution of the multiple-quantum coherence is refocused by two simultaneous π -pulses. The delays are set to $\tau_1 = 2.7$ ms ($\approx 1/4J(\text{NH})$), $\tau_2 = 15.1$ ms ($\approx 1/4J(\text{C}'\text{N})$), and $\delta = 1.3$ ms. The ^{15}N magnetization evolves during a semiconstant time period composed of two intervals RT (real time) and CT (constant time). Quadrature detection is achieved in ω_1 by the enhanced-sensitivity pulsed field gradient method. WALTZ-16 sequences are used to perform proton and nitrogen decoupling with radio frequency (RF) field strengths of 3.5 and 1.2 kHz, respectively. The phase cycle (16 steps) is $\phi_1 = 8(x, -x)$; $\phi_2 = 4(y)$, $4(-x)$, $4(-y)$, $4(x)$; $\phi_3 = 4(x)$, $4(y)$, $4(-x)$, $4(-y)$; $\phi_4 = 4(x, x, -x, -x)$; $\phi_5 = 4(y, y, -y, -y)$. For the selection of DQC or ZQC, $\phi_{\text{rec}} = 4(x, -x, -x, x)$ or $\phi_{\text{rec}} = 2(x, -x, -x, x, -x, x, x, -x)$, respectively. The duration of all sine-shaped gradients is 1 ms and their peak amplitudes are $g_{1x} = 31$, $g_{2y} = 20$, $g_{3z} = 19.5$, $g_{4x} = 45$, $g_{5z} = 30$, $g_{6z} = 39.5$, and $g_{7z} = -4$ G/cm.

4 Results and Discussion

Figure 2a shows some typical decay curves for TQC($C'_+N_+H_x^N$) and three-spin SQC($C'_+N_-H_x^N$) in nondeuterated ubiquitin. As expected, the decays are modulated by the homonuclear couplings $J(\text{H}^N\text{H}^\alpha)$ involving the amide and aliphatic protons, which were found to be about 8 Hz in agreement with measurements of Permi et al. [15]. Figure 3a shows the relatively poor correlation between $\Delta R(\text{TQC}/\text{SQC})$ rates measured in deuterated and nondeuterated samples (Table 1). The large errors associated with the rates measured in nondeuterated ubiquitin can be traced back to the Monte Carlo analysis of cosine modulated decays. The experimental signal-to-noise ratio was identical in all experiments for $\tau_m = 0$. Using a relaxation period τ_m that is a multiple of $1/J(\text{H}^N\text{H}^\alpha)$ would remove the modulations due to scalar couplings [12]. However, the TQC and three-spin SQC autorelaxation rates are much larger than $R_2 = 1/T_2$ of SQC, so that a constant delay $\tau_m = 1/J(\text{H}^N\text{H}^\alpha) \approx 125$ ms would lead to unacceptable losses in sensitivity.

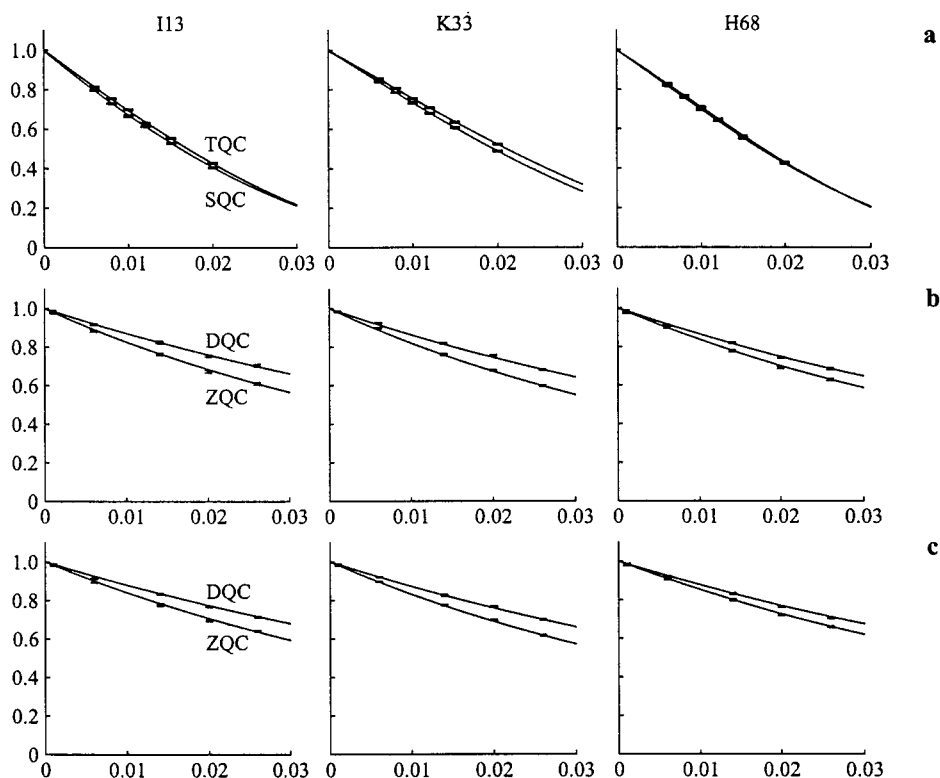


Fig. 2. Decay curves of multiple-quantum coherences in isoleucine 13, Lysine 33 and histidine 68 in ubiquitin (1.5 nM, pH 6.7, 300 K, 14 T) obtained by TQC/SQC experiments in nondeuterated ubiquitin (a), DQC/ZQC experiments in nondeuterated ubiquitin (b), and DQC/ZQC experiments in deuterated ubiquitin (c). Decays in a were fitted by a cosine modulated exponential function giving $J(\text{H}^{\text{N}}\text{H}^{\alpha})$ of about 8 Hz, whereas decays shown in b and c were fitted to mono-exponential functions.

Figure 2b and c shows similar decay curves of $\text{DQC}(C'_+N_+)$ and $\text{ZQC}(C'_+N_+)$ for nondeuterated and deuterated ubiquitin. As expected, the decays are mono-exponential in both cases.

Figure 4 shows the differences ΔR of the decay rates for all amino acids in the backbone of ubiquitin, comparing the earlier TQC/SQC method applied to deuterated ubiquitin, the DQC/ZQC method applied to the same deuterated sample, and the DQC/ZQC method applied to nondeuterated ubiquitin. It is clear that the latter rates are enhanced in magnitude (actually more negative) compared to those measured with the TQC/SQC method. Between the TQC/SQC and DQC/ZQC experiments, the enhancement is due to the dipolar contributions in Eq. (1). The contribution of the $C'H^{\text{N}}/NH^{\text{N}}$ dipole-dipole interference effect that is proportional to $J(0)$ is estimated to be -1.4 s^{-1} . Between deuterated and nondeuterated samples, the enhancement is due to dipole-dipole interactions in-

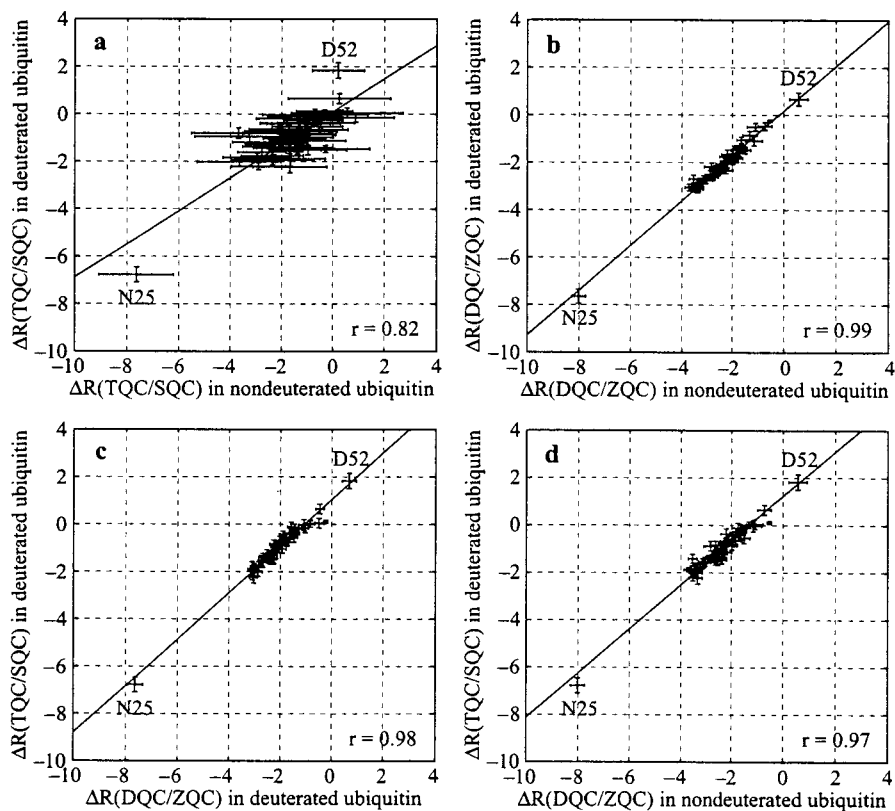


Fig. 3. **a** Correlation between $\Delta R(\text{TQC/SQC})$ in deuterated and nondeuterated ubiquitin ($r = 0.82$), **b** correlation between $\Delta R(\text{DQC/ZQC})$ in deuterated and nondeuterated ubiquitin ($r = 0.99$), **c** correlation between $\Delta R(\text{TQC/SQC})$ and $\Delta R(\text{DQC/ZQC})$ in deuterated ubiquitin ($r = 0.98$), **d** correlation between $\Delta R(\text{TQC/SQC})$ in deuterated ubiquitin and $\Delta R(\text{DQC/ZQC})$ in nondeuterated ubiquitin ($r = 0.97$).

Table 1. $\Delta R(\text{DQC/ZQC})$ and $\Delta R(\text{TQC/SQC})$ rates in nondeuterated and deuterated human ubiquitin (14.1 T, 300 K).

Residue	$\Delta R(\text{DQC/ZQC})$				$\Delta R(\text{TQC/SQC})$			
	Nondeuterated		Deuterated		Nondeuterated		Deuterated	
	ΔR	δ	ΔR	δ	ΔR	δ	ΔR	δ
L3	-1.984	0.161	-1.911	0.150	-1.344	1.234	-0.418	0.147
F4	-2.254	0.271	-2.332	0.131	-0.984	1.478	-1.126	0.225
V5	-1.501	0.225	-1.476	0.144	-1.007	1.380	-0.535	0.225
K6	-1.844	0.208	-1.470	0.195	-0.667	1.493	-0.371	0.107
T7	-2.171	0.275	-1.927	0.102	-2.068	1.202	-0.642	0.166
L8	-2.378	0.186	-2.308	0.120	-0.297	1.729	-1.463	0.152

Table 1 (continued).

Residue	$\Delta R(\text{DQC}/\text{ZQC})$				$\Delta R(\text{TQC}/\text{SQC})$			
	Nondeuterated		Deuterated		Nondeuterated		Deuterated	
	ΔR	δ	ΔR	δ	ΔR	δ	ΔR	δ
I13	-2.632	0.217	-2.268	0.155	-1.789	1.730	-0.825	0.176
T14	-1.545	0.138	-1.456	0.144	-1.349	1.651	-0.196	0.208
L15	-2.394	0.179	-2.122	0.163	-1.309	1.312	-0.984	0.141
V17	-3.057	0.263	-2.754	0.122	-0.978	1.520	-1.519	0.205
E18	-2.756	0.189	-2.606	0.133	-2.288	1.245	-1.378	0.173
S20	-2.899	0.199	-2.507	0.164	-1.455	1.125	-1.423	0.171
D21	-2.632	0.172	-2.430	0.096	-2.061	0.919	-1.417	0.161
T22	-1.725	0.232	-1.607	0.166	-1.049	1.336	-0.399	0.223
I23	-0.711	0.270	-0.470	0.160	0.240	1.995	0.651	0.209
N25	-8.023	0.272	-7.647	0.296	-7.641	1.433	-6.772	0.318
K27	-2.836	0.283	-2.176	0.166	-0.963	1.063	-0.876	0.204
A28	-3.596	0.141	-3.027	0.116	-2.319	0.985	-1.872	0.173
K29	-3.157	0.145	-2.692	0.139	-2.774	0.946	-1.604	0.208
I30	-3.548	0.168	-2.689	0.159	-1.251	1.243	-1.403	0.187
D32	-2.772	0.229	-2.516	0.147	-1.971	0.837	-1.288	0.218
K33	-2.548	0.165	-2.407	0.126	-1.384	0.925	-1.515	0.169
E34	-3.350	0.183	-3.055	0.147	-1.680	1.445	-2.226	0.254
G35	-3.392	0.222	-2.890	0.176	-3.655	1.631	-2.013	0.191
I36	-2.128	0.180	-1.758	0.135	-2.083	1.055	-0.734	0.125
Q40	-3.430	0.285	-3.042	0.126	-2.962	1.319	-1.830	0.182
Q41	-2.194	0.169	-1.772	0.097	-0.953	1.113	-0.728	0.157
L43	-1.090	0.331	-0.503	0.164	0.540	2.173	0.051	0.205
I44	-2.311	0.141	-1.936	0.156	-1.507	1.213	-1.046	0.171
F45	-1.151	0.336	-1.090	0.201	-0.704	2.051	-0.028	0.234
G47	-2.425	0.239	-2.048	0.120	-3.261	2.125	-0.955	0.251
K48	-3.716	0.171	-3.051	0.141	-2.882	0.933	-1.873	0.085
L50	-1.850	0.255	-1.833	0.160	-1.040	1.626	-0.665	0.220
D52	0.571	0.348	0.671	0.273	0.206	1.010	1.830	0.327
R54	-3.534	0.143	-3.096	0.132	-2.905	1.051	-2.205	0.141
T55	-3.416	0.234	-3.097	0.173	-2.362	1.611	-1.939	0.206
L56	-1.747	0.246	-1.591	0.138	-1.123	1.425	-0.105	0.202
E58	-3.246	0.203	-2.855	0.196	-2.370	1.218	-1.759	0.192
Y59	-3.377	0.215	-3.106	0.169	-1.659	1.362	-1.889	0.321
N60	-2.649	0.277	-2.265	0.145	-1.683	1.431	-1.430	0.237
I61	-2.199	0.236	-2.043	0.166	-1.727	1.159	-0.680	0.181
E62	-1.735	0.218	-1.380	0.095	-0.777	1.154	-0.266	0.156
K63	-2.202	0.223	-1.655	0.196	-0.479	1.334	-0.360	0.221
E64	-2.363	0.203	-2.306	0.139	-2.485	1.434	-1.190	0.208
S65	-2.678	0.198	-2.305	0.163	-2.426	0.998	-1.283	0.192
T66	-1.650	0.183	-1.051	0.132	0.875	1.501	-0.156	0.193
L67	-2.252	0.258	-1.753	0.107	-1.973	1.464	-0.730	0.193
H68	-1.639	0.169	-1.427	0.167	-1.298	1.547	-0.391	0.192
L69	-1.318	0.281	-0.849	0.178	0.308	1.551	0.024	0.146
V70	-1.982	0.218	-1.952	0.126	-3.683	1.842	-0.805	0.230
G76	-0.521	0.066	-0.239	0.047	-0.335	1.098	0.118	0.057

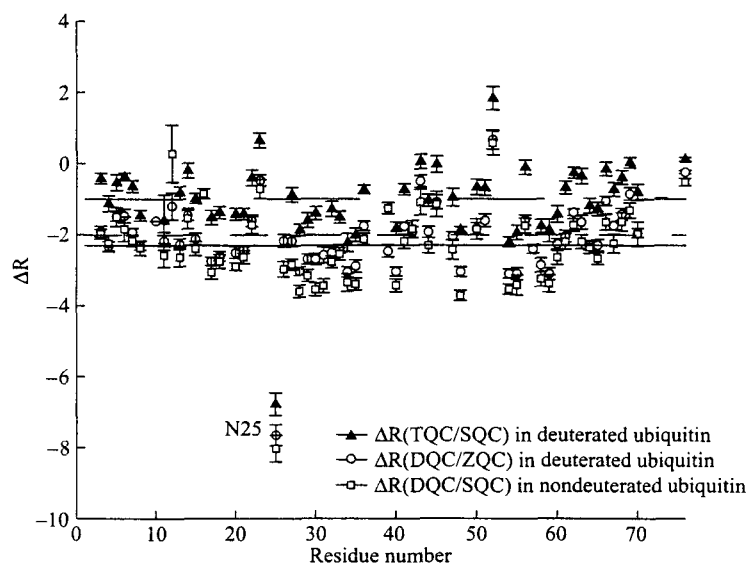


Fig. 4. Triangles represent the rates $\Delta R(\text{TQC}/\text{SQC})$ in deuterated ubiquitin. Circles and squares represent the rates $\Delta R(\text{DQC}/\text{ZQC})$ in deuterated and nondeuterated ubiquitin. The horizontal lines indicate the mean values for each of the three experiments.

volving the C' and N nuclei and external H^α protons, which contribute on average about -0.32 s^{-1} . Experimentally, as shown in Fig. 4, the first contribution is found to be -1.1 s^{-1} , while the second one contributes -0.25 s^{-1} on average.

The correlation between the rates $\Delta R(\text{DQC}/\text{ZQC})$ in deuterated and nondeuterated ubiquitin was found to be excellent ($r = 0.99$), as shown in Fig. 3b. Figure 3c shows a very good correlation ($r = 0.98$) when the SQC/TQC and ZQC/DQC experiments are applied to the same deuterated sample.

In spite of the strong dipolar contributions in the nondeuterated sample, the measured rates $\Delta R(\text{DQC}/\text{ZQC})$ permit the identification of residues that experience significant conformational exchange, such as asparagine 25 [10]. Figure 3d shows the very good correlation ($r = 0.97$) between the rates obtained by applying the sophisticated TCQ/SQC experiment to (expensive) deuterated ubiquitin and the rates obtained with the simple DQC/ZQC experiment in (cheap) nondeuterated ubiquitin.

5 Conclusions

The excellent agreement between the rates $\Delta R(\text{TQC}/\text{SQC})$ in deuterated ubiquitin and the rates $\Delta R(\text{DQC}/\text{ZQC})$ in nondeuterated ubiquitin makes it possible to use the latter to identify residues experiencing slow backbone motions. This does not require any deuterated samples and should greatly simplify the separation

of CSM/CSM and CSA/CSA effects by multiple refocusing, since only two nuclei (instead of three) must be simultaneously refocused. The $\Delta R(DQC/ZQC)$ rates have also been determined successfully in the much larger major urinary protein (MUP) with 162 amino acids and a correlation time of ca. 8 ns at 308 K [16]. These measurements provide evidence that some residues experience increased mobility upon binding to pheromones, as will be described elsewhere.

Acknowledgments

We are indebted to Dominique Frueh for useful discussions. This work has been supported by the European Commission (Research Training Network on Cross-correlations), the Fonds National de la Recherche Scientifique (FNRS, Switzerland), the Commission pour la Technologie et l'Innovation (CTI, Switzerland), and the Centre National de la Recherche Scientifique (CNRS, France).

References

1. Millet O., Loria J.P., Kroenke C.D., Pons M., Palmer A.G.: *J. Am. Chem. Soc.* **122**, 2867–2877 (2000)
2. Mulder F.A.A., Skrynnikov N.R., Hon B., Dahlquist F.W., Kay L.E.: *J. Am. Chem. Soc.* **123**, 967–975 (2001)
3. Mulder F.A.A., Akke M.: *Magn. Reson. Chem.* **41**, 853–865 (2003)
4. Chiarparin E., Rüdiger S., Bodenhausen G.: *ChemPhysChem* **2**, 41–45 (2001)
5. Dittmer J., Kim C.-H., Bodenhausen G.: *J. Biomol. NMR* **26**, 259–275 (2003)
6. Frueh D., Tolman J.R., Bodenhausen G., Zwaalen C.: *J. Am. Chem. Soc.* **123**, 4810–4816 (2001)
7. Vugmeyster L., Perazzolo C., Wist J., Frueh D., Bodenhausen G.: *J. Biomol. NMR* **28**, 173–177 (2004)
8. Carr H.Y., Purcell E.M.: *Phys. Rev.* **94**, 630–638 (1954)
9. Meiboom S., Gill D.: *Rev. Sci. Instrum.* **29**, 688–691 (1958)
10. Wist J., Frueh D., Tolman J., Bodenhausen G.: *J. Biomol. NMR* **28**, 263–272 (2004)
11. Dittmer J., Bodenhausen G.: *J. Am. Chem. Soc.* **126**, 1314–1315 (2004)
12. Pellecchia M., Pang Y., Wang L., Kurochkin A.V., Kumar A., Zuiderweg E.R.P.: *J. Am. Chem. Soc.* **121**, 9165–9170 (1999)
13. Delaglio F., Grzesiek S., Vuister G.W., Zhu G., Pfeifer J., Bax A.: *J. Biomol. NMR* **6**, 277–293 (1995)
14. Bevington P., Robinson D.: *Data Reduction and Error Analysis for the Physical Sciences*, 2nd edn. New York: McGraw-Hill 1992.
15. Permi P., Kilpeläinen I., Heikkinen S.: *Magn. Reson. Chem.* **37**, 821–826 (1999)
16. Bingham R.J., Findlay J.B.C., Hsieh S.-Y., Kalverda A.P., Kjellberg A., Perazzolo C., Phillips S.E.V., Seshadri K., Trinh C.H., Turnbull W.B., Bodenhausen G., Homans S.W.: *J. Am. Chem. Soc.* **126**, 1675–1681 (2004)

Authors' address: Geoffrey Bodenhausen, Département de chimie, associé au CNRS, Ecole Normale Supérieure, 24 rue Lhomond, 75231 Paris cedex 05, France